Investigation on Corrosion Resistance of Welded Cu-Bearing 304L Stainless Steel Against *Pseudomonas aeruginosa*

Lu Yin[1,2†], Tong Xi[1†], Chunguang Yang[1]*, Jinlong Zhao[1], Yupeng Sun[1], Hanyu Zhao[1] and Ke Yang[1]

[1] Institute of Metal Research, Chinese Academy of Sciences, Shenyang, China, [2] School of Materials Science and Engineering, University of Science and Technology of China, Shenyang, China

In this work, the microbiologically influenced corrosion (MIC) behaviors of welded 304L stainless steel (304L SS) and Cu-bearing 304L SS (304L-Cu SS) in a *Pseudomonas aeruginosa* culture medium were comparatively studied. Open circuit potential (OCP), linear polarization resistance (LPR), electrochemical impedance spectroscopy (EIS), and potentiodynamic polarization were employed to characterize the corrosion behavior of the (welded) steel substrates. The biofilm morphology and the live/dead staining condition of the sessile cells were observed by scanning electron microscopy (SEM) and confocal laser scanning microscopy (CLSM). And the pitting corrosion was investigated with a 3D mode of CLSM. The experimental results showed that the copper (Cu) addition had no obvious influence on the microstructure of 304L SS in welding zones (WZs) and base metal. The WZs of 304L SS and 304L-Cu SS in sodium chloride solution possessed a lower pitting potential and a higher corrosion current density. However, owing to the continuous release of Cu ions, inhibiting the excretion of corrosive extracellular polymeric substances (EPSs) and the extracellular electron transport (EET) process, both the localized and uniform corrosion attack induced by the *P. aeruginosa* biofilm was significantly reduced. In comparison with that of 304L SS, the corrosion resistance of 304L-Cu SS in the WZ against *P. aeruginosa* was obviously higher.

Keywords: Cu-bearing stainless steels, tungsten inert gas welding, microbiologically influenced corrosion, confocal laser scanning microscopy, pitting corrosion

INTRODUCTION

The 304L stainless steel (SS) has been widely used in many fields such as food industry, medical device, transportation, and daily appliance, owing to its excellent combination of mechanical properties, corrosion resistance, and workability (Nie et al., 2011; Zhang et al., 2013). In some of those application conditions, the steel needs to be welded before use. Nevertheless, welding joints of steels are usually recognized as sensitive zones to corrosion. This is because the welding zone (WZ) of austenitic SSs has a microstructure of a dendritic austenite matrix with a small amount of δ-ferrite (Dadfar et al., 2007; Moon et al., 2011). And the formation of δ-ferrite under the pseudo-equilibrium condition in austenitic SSs may cause Cr-depleted zones and lead to

localized corrosion (Lu et al., 2005). More seriously, the corrosion that occurred in the sensitive zones could be severely aggravated by corrosive microorganisms in service environments, which is named as microbiologically influenced corrosion (MIC; Neria-Gonzalez et al., 2006; Aktas et al., 2010; Huttunen-Saarivirta et al., 2012). According to the literatures, MIC accounts for 20% of all corrosion damages (Zhang et al., 2015; Xu et al., 2017a; Hashemi et al., 2018; Li et al., 2018). The formation of corrosive biofilm on metal surface changes the electrochemical conditions and thus accelerates both uniform and pitting corrosions (Vigneron et al., 2016; Skovhus et al., 2017).

As a new kind of structural and functional integrated metal material, the Cu-bearing SSs have been developed and attracted great attention in recent years (Jin et al., 2016; Jiang et al., 2016; Xi et al., 2016, 2017). By adding a proper amount of copper (Cu) into a steel matrix, trace amount of Cu ions could be continuously released in application environment, thus offering an antibacterial function for the SSs (Nan and Yang, 2010). Previous works have confirmed that the Cu-bearing SSs possessed excellent antibacterial property against *Porphyromonas gingivalis*, *Staphylococcus aureus*, and so forth (Zhang et al., 2013). It was reported that Cu-bearing SSs also showed a significant beneficial effect on MIC. Nan et al. (2015) confirmed that Cu-bearing 304L SS (304L-Cu SS) had higher resistance against MIC. Therefore, applying Cu-bearing SS to replace the commonly used SS could be a feasible solution to inhibit the MIC attack in some harsh corrosive environments (Li et al., 2015).

Pseudomonas aeruginosa, the aerobic Gram-negative bacterium, is a kind of typical corrosive bacteria, which are widely distributed in various types of water environments (Hamzah et al., 2013). In recent years, many researches proved that *P. aeruginosa* can induce the pitting corrosion of carbon steels and SSs (Hamzah et al., 2013; Wadood et al., 2017). Although there were some studies related to the influence of Cu-bearing SSs on MIC behaviors, a comparison between a steel matrix and WZ of Cu-bearing SS and the relevant effect on the MIC behavior are still lacking of enough understanding. Hence, the purpose of this work is to comparatively investigate the difference on corrosion behavior between the WZs and a matrix of 304L SS and 304L-Cu SS in a *P. aeruginosa* culture medium by means of linear polarization, electrochemical impedance spectroscopy (EIS), potentiodynamic polarization, and confocal laser scanning microscopy (CLSM).

MATERIALS AND METHODS

Materials

In this work, 304L SS and 304L-Cu SS were melted in a 25-kg vacuum smelting furnace. The ingots were hot rolled into plate shape with a thickness of 4 mm and then finally cold rolled into 1-mm-thick sheets. Chemical compositions of the 304L SS and 304L-Cu SS are listed in **Table 1**. Both 304L SS and 304L-Cu SS were solution treated at 1,050°C for 0.5 h and followed by quenching in water. Afterward, a tungsten inert gas (TIG) welding was employed to weld the SS sheets together. Selected welding parameters were 93 A of welding current and

52 cm/min of welding speed. The WZs and base metal (BM) specimens of 304L SS and 304L-Cu SS were separately cut off and then machined into square coupons with dimensions of 10 mm $\times$ 10 mm $\times$ 1 mm. Among them, the coupons for making electrodes were sealed with epoxy resin and silica gel, leaving an exposed working area of 1 cm^2. Each working surface for electrochemical measurements and immersion tests was polished to a 1,000-grit finish with metallographic sandpaper, then cleaned with absolute ethyl alcohol, and finally dried in hot air stream. The 75% (v/v) alcohol and ultraviolet (UV) light were used to sanitize the specimens and electrodes just before the experiment. The surfaces for microstructure analysis were polished to a mirror finish and electro-etched at a 2 V of direct current in 60% (v/v) nitric acid solution for 15 s and then observed by the metallurgical microscope (Z1 M, Zeiss, Germany).

Culture Medium and Inoculum

Pseudomonas aeruginosa (1A00099) was purchased from the Marine Culture Collection of China (MCCC) and cultured in the 2216E medium in this work. The 2216E culture medium was composed of following compounds: 3.24 g/L of Na_2SO_4, 1.8 g/L of $CaCl_2$, 0.55 g/L of KCl, 0.16 g/L of Na_2CO_3, 0.08 g/L of $SrBr_2$, 0.022 g/L of H_3BO_3, 0.004 g/L of $NaSiO_3$, 0.0024 g/L of NaF, 0.0016 g/L of NH_4NO_3, 0.008 g/L of NaH_2PO_4, 5.0 g/L of peptone, 1.0 g/L of yeast extract, and 0.1 g/L of ferric citrate. The pH value of 2216E was adjusted to 7.2 $\pm$ 0.2. The cultural temperature was controlled at 37°C during the testing period, which was favorable to *P. aeruginosa* growth.

Electrochemical Measurements

To compare the corrosion resistance difference of 304L SS BM, 304L SS WZ, 304L-Cu SS BM, and 304L-Cu SS WZ, the polarization curves were measured with a three-electrode system in 3.5 wt.% of NaCl solution by using the electrochemical workstations (Reference 1000TM, Gamry Instruments, United States). The measured specimen was the working electrode in a three-electrode system; a saturated calomel electrode (SCE) and a platinum electrode were used as the reference electrode and the counter electrode, respectively. Prior to polarization curve measurements, the open circuit potential (OCP) was monitored at least 30 min until its value was relatively stable. In addition, linear polarization resistance (LPR) and EIS were chosen to monitor the change of corrosion resistance for different electrodes during the 14 days of testing period in the culture medium with presence of *P. aeruginosa*.

Linear polarization resistance measurements were conducted at a scan rate of 0.125 mV/s within the range of $\pm$ 5 mV versus E_{OCP}. The EIS measurements were performed at a sinusoidal voltage signal of 10 mV in the frequency range from 10^5 to 10^{-2} Hz. And the impedance results were fitted by using ZSimpWin software with two reasonable equivalent circuit models. After 14 days, potentiodynamic polarization measurements were scanned from -250 to 600 mV versus E_{OCP} (the maximum current limit was 1 mA/cm^2) at a potential sweep rate of 0.5 mV/s (Li et al., 2016, 2017; Xu et al., 2017b; Liu et al., 2018a,b; Sun et al., 2019).

TABLE 1 | Chemical compositions of 304L and 304L-Cu SS (wt.%).

	C	Si	Mn	Ni	Cr	Cu	Fe
304L SS	0.006	0.45	1.34	8.72	18.09	–	Balance
304L-Cu SS	0.008	0.42	1.541	8.55	17.95	4.10	Balance

SS, stainless steel.
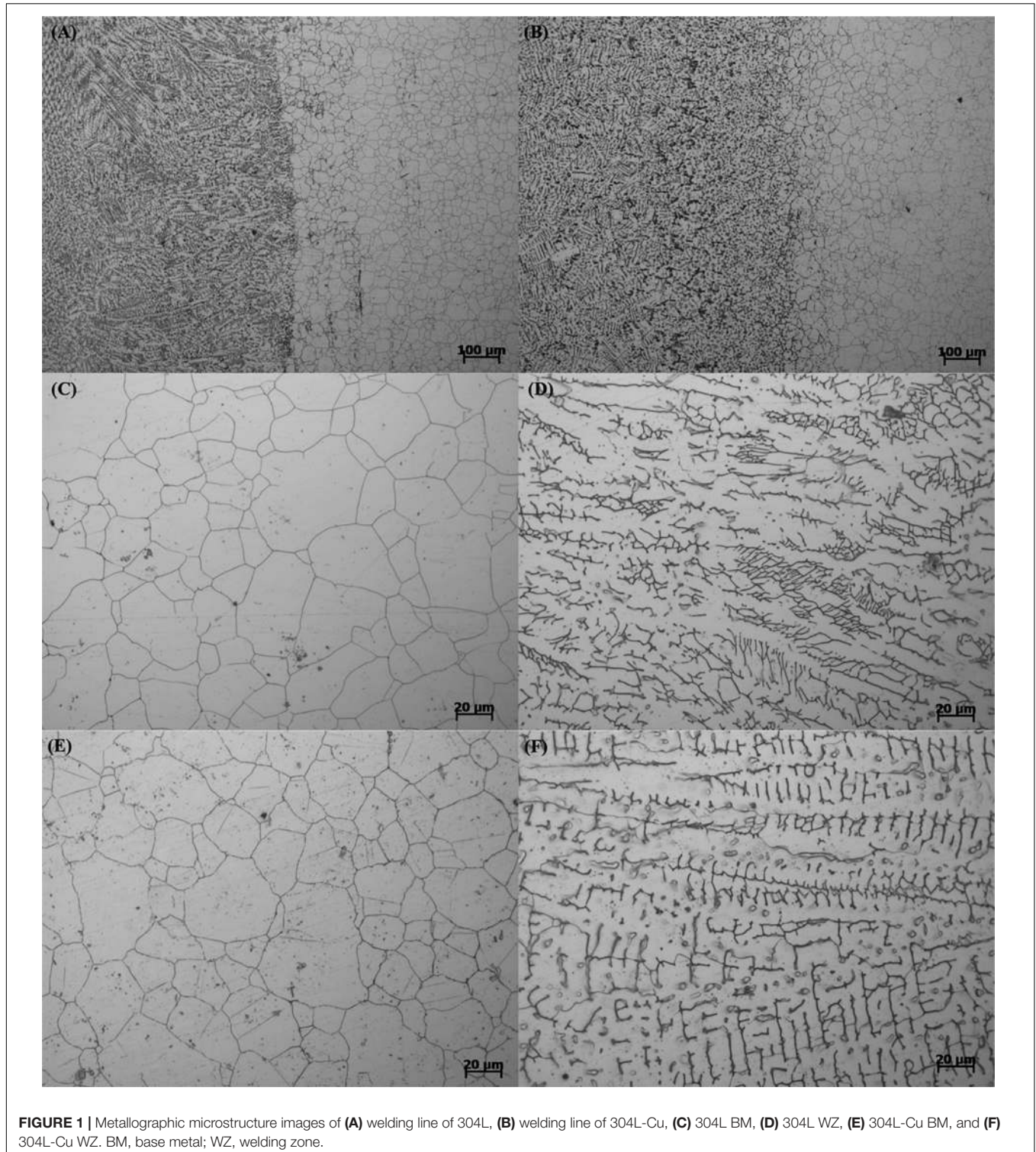
FIGURE 1 | Metallographic microstructure images of **(A)** welding line of 304L, **(B)** welding line of 304L-Cu, **(C)** 304L BM, **(D)** 304L WZ, **(E)** 304L-Cu BM, and **(F)** 304L-Cu WZ. BM, base metal; WZ, welding zone.
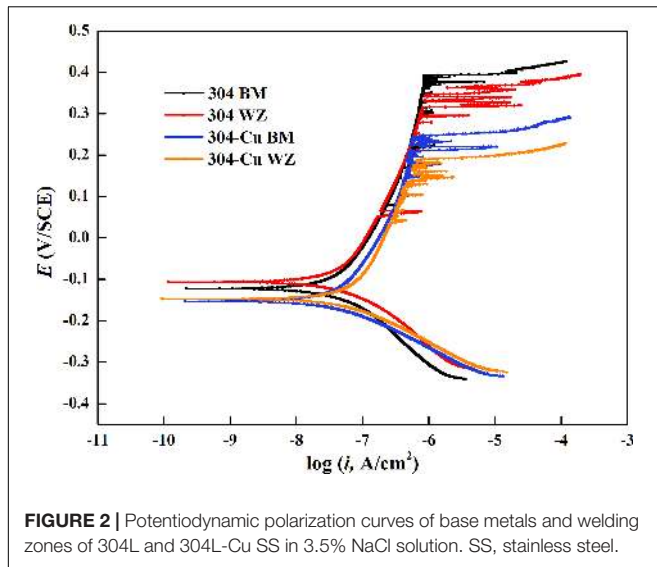
FIGURE 2 | Potentiodynamic polarization curves of base metals and welding zones of 304L and 304L-Cu SS in 3.5% NaCl solution. SS, stainless steel.

TABLE 2 | Fitting results derived from the potentiodynamic polarization curves in **Figure 2**.

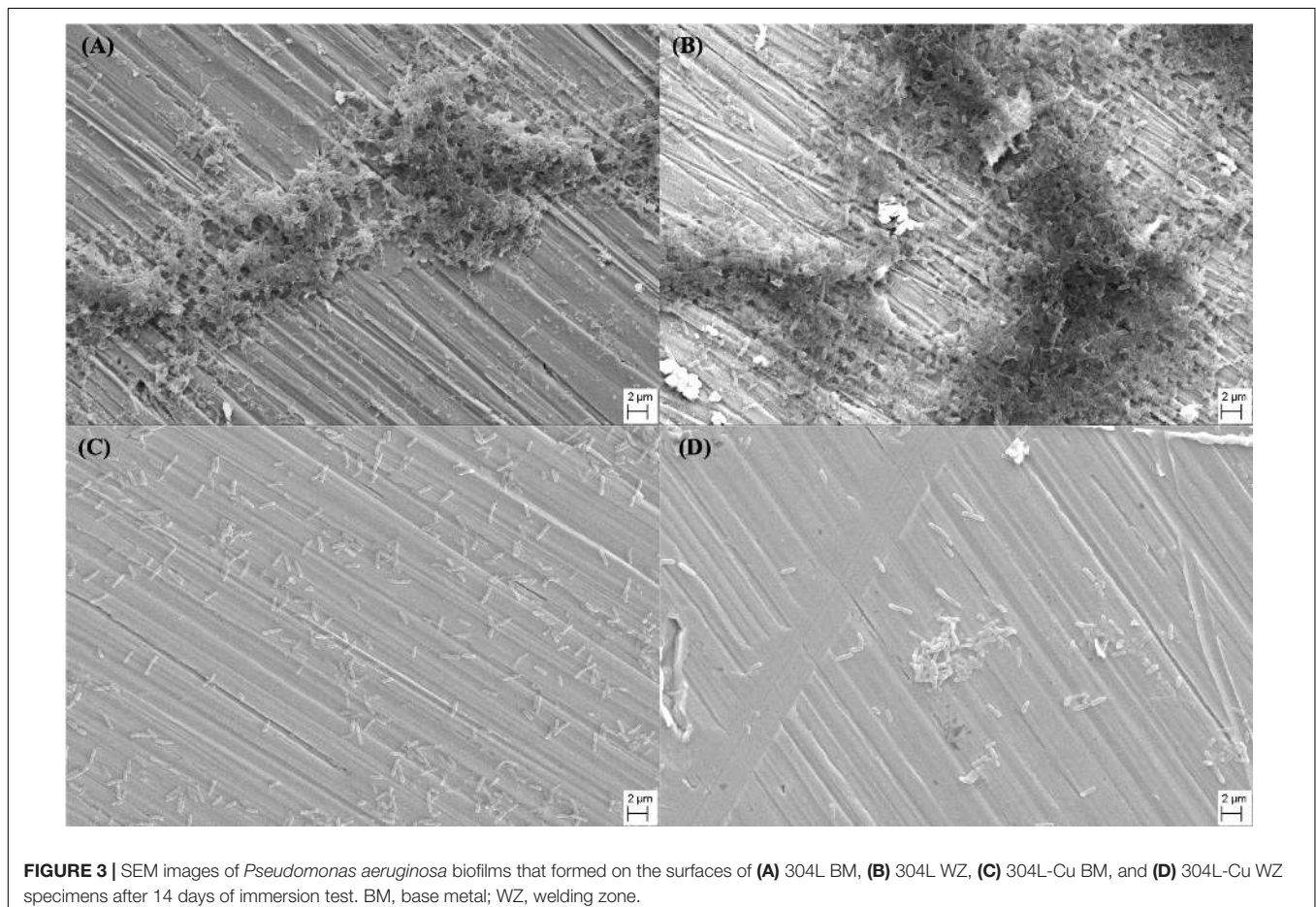|	E_{corr} (mV/SCE)	I_{corr} (nA/cm^2)	I_{pass} (nA/cm^2)	E_{pit} (mV/SCE)
304L BM	−122.1	55.2	285.8	393.5
304L WZ	−106.5	57.5	316.2	327.2
304L-Cu BM	−153.1	41.3	338.1	264.6
304L-Cu WZ	−147.7	45.5	358.9	210.3

SCE, saturated calomel electrode; BM, base metal; WZ, welding zone.

of specimens. Those biofilms were fixed by using 2.5% (v/v) glutaraldehyde solution for 8 h and dehydrated by ethanol–water solutions successively with the concentrations of 30, 40, 50, 60, 70, 80, 90, 95, and 100 and then sputter-coated with gold to improve conductivity of the observing surfaces.

A CLSM (Model C2 Plus, Nikon, Japan) was used to further characterize the survival condition of *P. aeruginosa* cells in biofilm. Before the observation, all the surfaces were stained using following steps: firstly, the surfaces were cleaned with phosphate-buffered saline (PBS) to remove scum and planktonic cells and then stained using SYTO-9 and propidium iodide (PI; Invitrogen, Eugene, OR, United States).

Surface and Biofilm Analysis

After the immersion tests, a field emission scanning electron microscopy (FE-SEM, Ultra-plus, Zeiss, Germany) was used to observe the *P. aeruginosa* biofilms formed on the surface
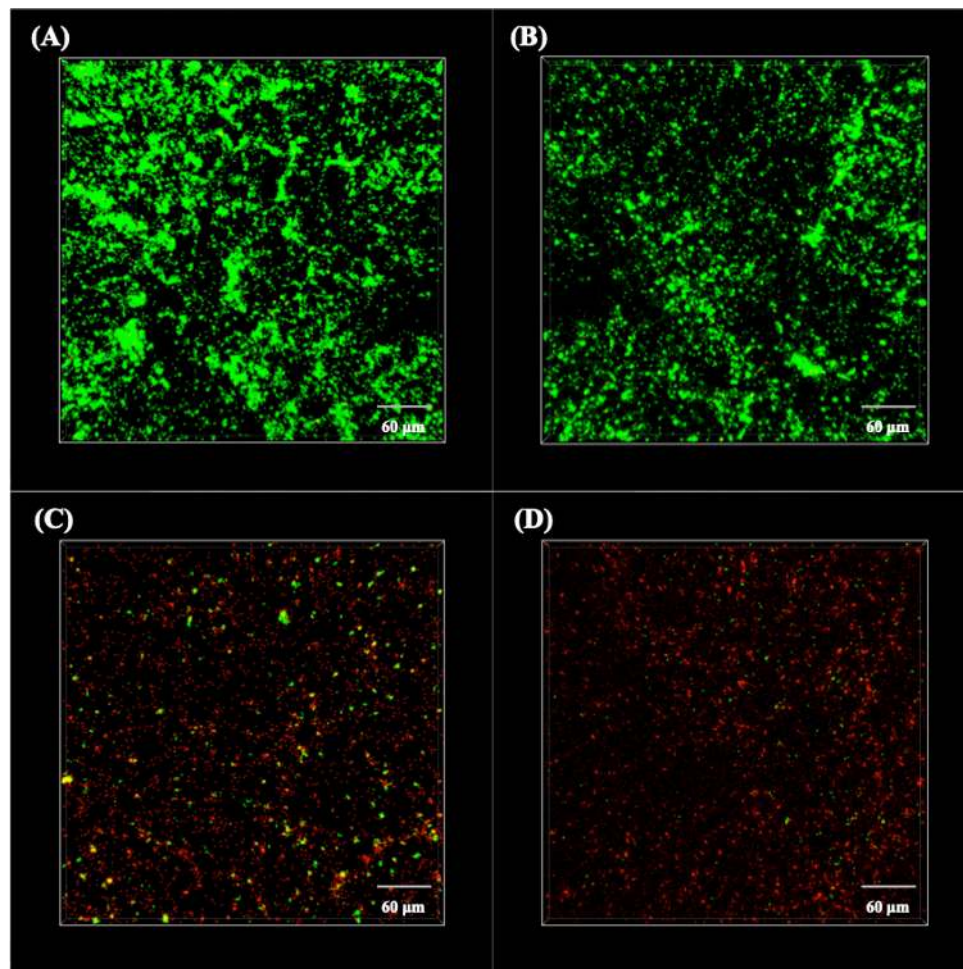

FIGURE 3 | SEM images of *Pseudomonas aeruginosa* biofilms that formed on the surfaces of **(A)** 304L BM, **(B)** 304L WZ, **(C)** 304L-Cu BM, and **(D)** 304L-Cu WZ specimens after 14 days of immersion test. BM, base metal; WZ, welding zone.

FIGURE 4 | CLSM images of live/dead stained *Pseudomonas aeruginosa* biofilms on the surfaces of **(A)** 304L BM, **(B)** 304L WZ, **(C)** 304L-Cu BM, and **(D)** 304L-Cu WZ specimens after 14 days of immersion test. CLSM, confocal laser scanning microscopy; BM, base metal; WZ, welding zone.

The live cells can be stained with SYTO-9, whereas the dead cells can be stained with PI. All the live cells can be observed as green dots under CLSM with the wavelength of 488 nm, and the red dots with the wavelength of 559 nm represent the dead cells.

After the biofilms and corrosion products were removed (Li et al., 2016), the corrosion pitting induced by *P. aeruginosa* was observed with CLSM (LSM 710, Zeiss, Germany). The depth of pits was measured with the 3D mode of CLSM.

RESULTS

Microstructure Observation and Corrosion Resistance

Figure 1 shows the microstructures of the whole welding joint, BM, and WZ of 304L SS and 304L-Cu SS. As displayed in **Figure 1**, no significant difference was observed between 304L SS and 304L-Cu SS. The microstructures of BM for 304L SS and 304L-Cu SS consisted of fully austenite grains, with the grain size of about $\sim$35 μm, whereas the WZ microstructures were composed of a dendritic austenite matrix decorated with a small number of δ-ferrite (Pouranvari et al., 2015).

Figure 2 shows the potentiodynamic polarization curves of BM and WZ from 304L SS and 304L-Cu SS in 3.5% NaCl solution. The values of corrosion potential (E_{corr}), pitting potential (E_{pit}), corrosion current density (I_{corr}), and passivation current density (I_{pass}) were derived and listed in **Table 2**. It is obvious that Cu addition led to a negative shift of E_{corr} and a slightly decrease of I_{corr} from 55.2 nA/cm^2 of 304L BM to 41.3 nA/cm^2 of 304L-Cu BM. However, the E_{pit} of 304L-Cu BM was much lower than that of 304L BM with values of 246.6 and 393.5 mV, respectively. Meanwhile the I_{pass} value was increased from 285.8 nA/cm^2 of 304L BM to 338.1 nA/cm^2 of 304L-Cu BM. 304L-Cu WZ had the lowest E_{pit} value and the highest I_{pass} value among all electrodes, which were 210.3 mV/SCE and 358.9 nA/cm^2, respectively. Of note, the increased I_{pass} and I_{corr} and reduced E_{pit} values of 304L WZ and 304L-Cu WZ indicated the lower corrosion resistance than that of BM specimens.
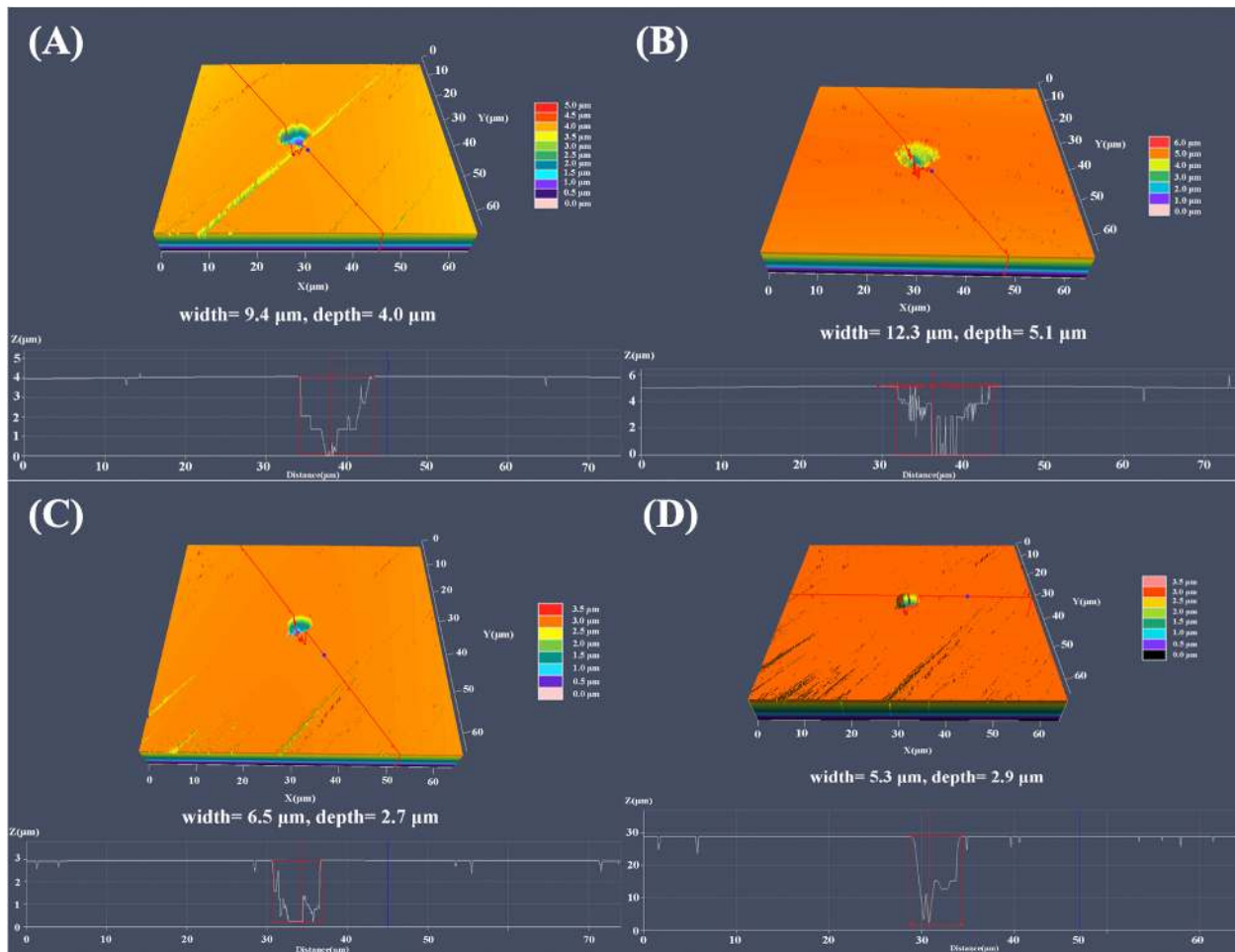
FIGURE 5 | Largest pit depth measured by CLSM of **(A)** 304L BM, **(B)** 304L WZ, **(C)** 304L-Cu BM, and **(D)** 304L-Cu WZ in the *Pseudomonas aeruginosa*-inoculated culture medium after 14 days. CLSM, confocal laser scanning microscopy; BM, base metal; WZ, welding zone.

Surface and Biofilm Analysis

SEM images shown in **Figure 3** depict the morphology of the *P. aeruginosa* biofilms on different specimen surfaces after 14 days of immersion in culture medium. For both 304L SS BM and 304L SS WZ (shown in **Figures 3A,B**, respectively), the amounts of sessile *P. aeruginosa* cells on their surfaces were much larger than those on Cu-bearing specimen surfaces (shown in **Figures 3C,D**). And the *P. aeruginosa* biofilms formed on 304L SS BM and 304L SS WZ were obviously more compact and concentrated compared with those on Cu-bearing BM and WZ specimens.
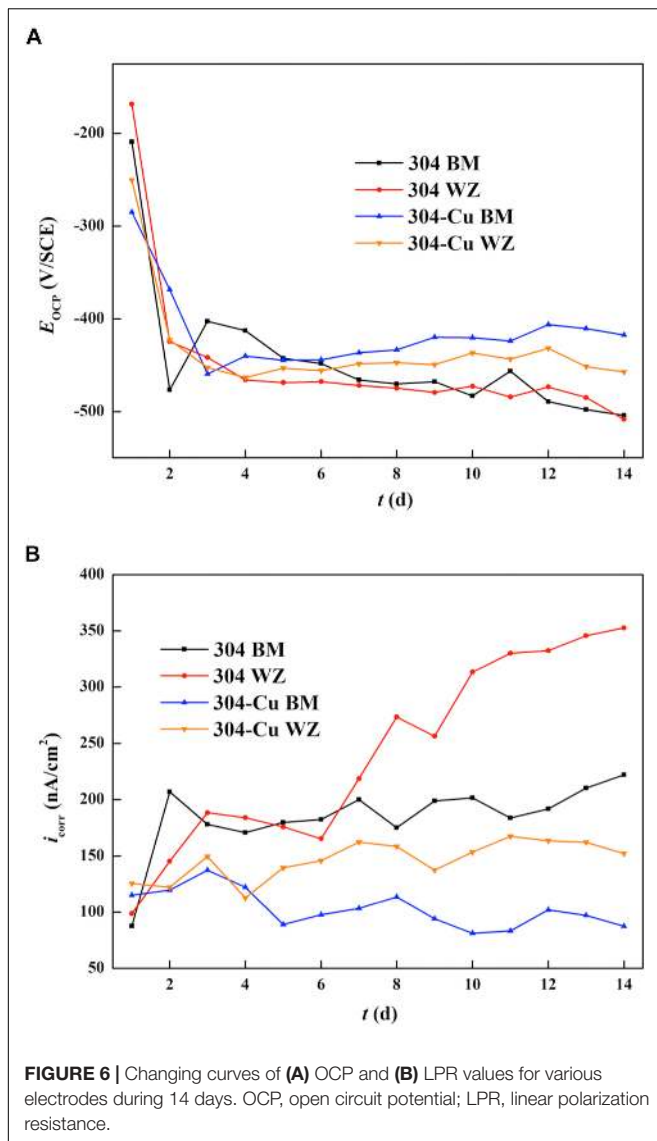
To further detect the activation of the sessile *P. aeruginosa* cells, the biofilms were stained with SYTO-9 and PI and then observed under CLSM at wavelengths of 488 and 559 nm, respectively. The live/dead staining images are shown in **Figure 4**. It is obvious that almost all sessile *P. aeruginosa* cells on the surfaces of 304L BM and 304L WZ (shown in **Figures 4A,B**) were alive. However, plenty of dead cells appeared on the Cu-bearing specimen surfaces (shown in **Figures 4C,D**). In addition, the distribution of attached cells

on each specimen imaged by CLSM consisted with that observed by SEM.

Figure 5 shows the analysis results of the maximum pit depth with the CLSM in 3D mode. As shown in **Figure 5B**, the most severe pitting corrosion was observed on 304L WZ specimen, with maximum pit of 5.1 μm in depth and 12.3 μm in width. The maximum depth of pit found on the surface of 304L BM reached 4.9 μm, which was deeper than that of Cu-bearing specimens. The most serious pits found on 304L-Cu BM and 304L-Cu WZ were 2.7 and 2.9 μm in depth, respectively.

Electrochemical Measurements

Figure 6A shows the E_{OCP} curves of four types of electrodes varying with immersion time in *P. aeruginosa* culture medium. The variation tendency of each curve reveals that the most significant changes in E_{OCP} values occurred in the initial stage of the immersion test. The initial E_{OCP} values of 304L BM and 304L WZ were higher than those of the Cu-bearing electrodes, which were −209.1 and −168.5 mV/SCE, respectively. However, after the sharp decline stage, the values of 304L BM and 304L

FIGURE 6 | Changing curves of (A) OCP and (B) LPR values for various electrodes during 14 days. OCP, open circuit potential; LPR, linear polarization resistance.

WZ peaked around −470.1 and −474.8 mV/SCE at about 7 days and afterward maintained a relatively slow decline. After 14 days of immersion, the E_{OCP} of 304L BM and 304L WZ was similar, which was −504.0 and −508.4 mV/SCE, respectively. Compared with those of 304L SS, the E_{OCP} changes of Cu-bearing electrodes were smaller in the sharp decline stage. The initial values for E_{OCP} of 304L-Cu BM and 304L-Cu WZ were −284.9 and −250.3 mV/SCE, respectively. But the final E_{OCP} value of 304L-Cu BM at the 14 days was the highest among the four electrodes, which was −417.5 mV/SCE. Even the E_{OCP} of 304L-Cu WZ was still higher than that of 304L-Cu BM and 304L-Cu WZ after 14 days of immersion.

Figure 6B shows the variation of I_{corr} values (measured by LPR tests) as a function of immersion time. The I_{corr} can directly reflect the uniform corrosion rate of the electrode. The initial I_{corr} values of 304L BM, 304L WZ, 304L-Cu BM, and 304L-Cu WZ were 87.6, 98.7, 115.2, and 125.5 nA/cm^2, respectively. It indicated that the corrosion resistance at the incomplete

formation stage of *P. aeruginosa* biofilm for each electrode was consistent with the measuring results in 3.5% NaCl solution. With the biofilm growth on the surface of electrodes, the I_{corr} values of 304L BM and 304L WZ electrodes experienced a continuous increase during the whole immersion period owing to the formation of *P. aeruginosa*. But for 304L-Cu BM and 304L-Cu WZ electrodes, the I_{corr} remained unchanged at later immersion time. At 14 days, the I_{corr} values of 304L BM, 304L WZ, 304L-Cu BM, and 304L-Cu WZ electrodes became 222.0, 352.7, 87.3, and 152.1 nA/cm^2, respectively. 304L WZ showed the worst corrosion resistance among of all electrodes owing to the influence of *P. aeruginosa* biofilm. Obviously, 304L-Cu WZ and 304L-Cu BM possessed the better corrosion resistance than 304 WZ and 304 BM.

Figure 7 shows the Nyquist and Bode plots of four types of experimental electrodes in the *P. aeruginosa* culture medium. It can be found that the measured impedance plots were different, depending on the exposure time and the Cu addition. To compare the detailed impedance parameters, the EIS data were fitted with appropriate equivalent circuits as shown in **Figure 8**, where R_s represents the culture medium resistance; R_f and Q_f account for the resistance and capacitance of the surface film, respectively; and R_{ct} and Q_{dl} denote the electron transfer resistance of passivation film and double layer capacitance, respectively. In this work, the capacitance C was replaced by the constant phase element (CPE, Q) because of the heterogeneity of the experimental electrode upon corrosion in the culture medium; thus, the ideal capacitance element was not good for fitting the corroded SS electrode (Liu et al., 2017). The expression for the CPE is

$$Z_Q = Y_0^{-1}(j\omega)^{-\alpha}$$

where ω is the angular frequency (rad/s) and Y_0 and α are the coefficients reflecting the deviation of electrode from the ideal reaction model. Based on the shape of Bode plots and the images of SEM observation, the data of all electrodes at the first day were fitted with the equivalent circuit shown in **Figure 8A**, whereas other data were fitted with the equivalent circuit in **Figure 8B**. In the fitting process, all χ^2 values were lower than 10^{-4}, which means that fitting error was small. The black solid fitting lines in Nyquist and Bode also show the high coincidence degree. Through the diameter change of capacitance loops and the fitted values of R_f and R_{ct}, the corrosion resistance of each electrode during testing period can be evaluated. The initial fitted R_{ct} values of 304L BM, 304L WZ, 304L-Cu BM, and 304L-Cu WZ were 295.5, 262.6, 226.1, and 206.3 kΩ/cm^2, respectively. At the 14 days, the sum of fitted R_f and R_{ct} of 304L BM, 304L WZ, 304L-Cu BM, and 304L-Cu WZ changed to 117.2, 73.7, 218.6, and 176.4 kΩ/cm^2, respectively. The tendency and conclusion were consistent with the LPR results.

Figure 9 shows the potentiodynamic polarization curves of the four types of electrodes after 14 days of immersion in the 2216E culture medium inoculated with *P. aeruginosa*. It can be seen that each electrode was still kept in the passivation state after immersion in this corrosive environment. 304L WZ had the largest corrosion I_{corr} value (877.0 nA/cm^2) and the lowest E_{pit} value (212.8 mV/SCE). As the E_{pit} value reflects
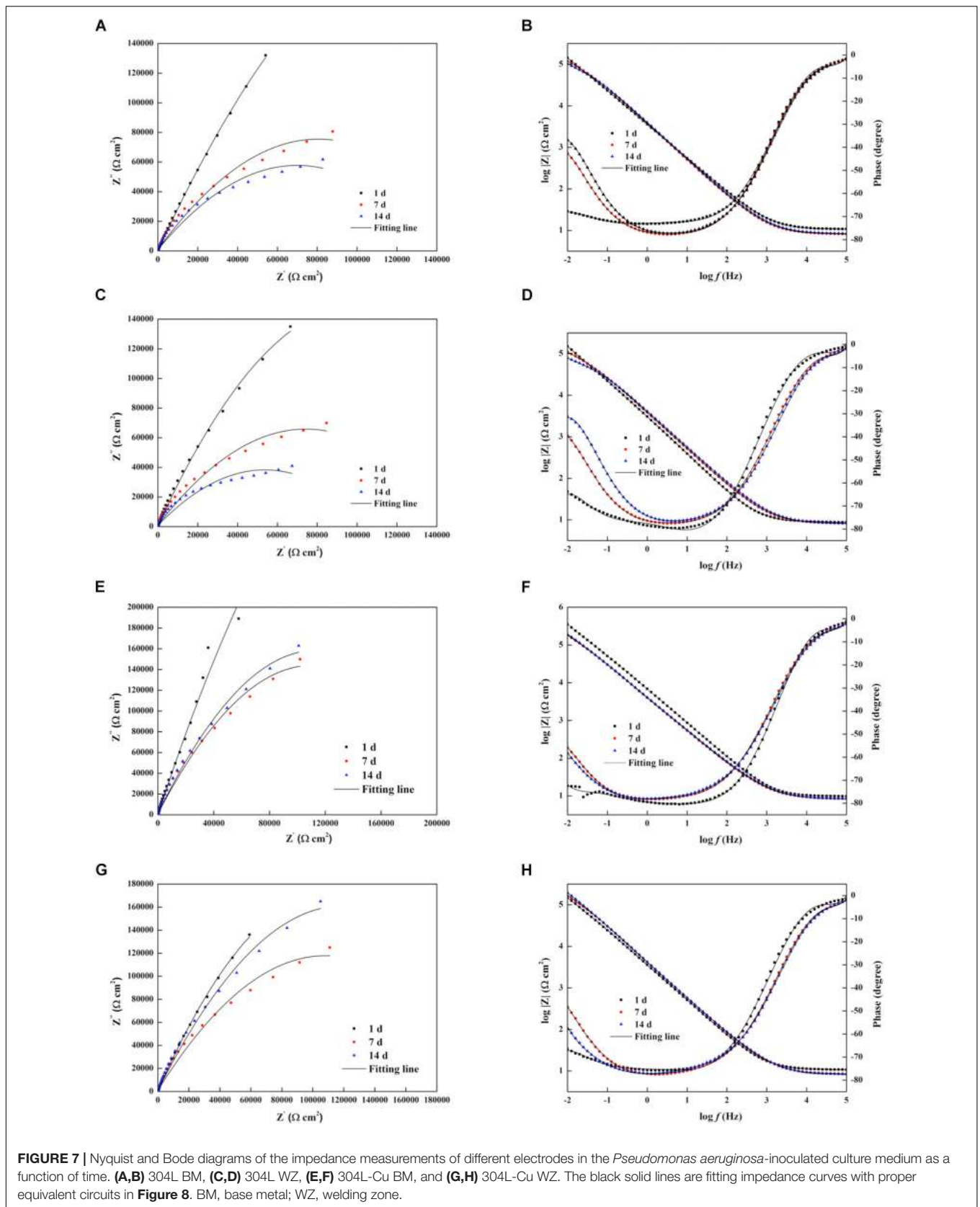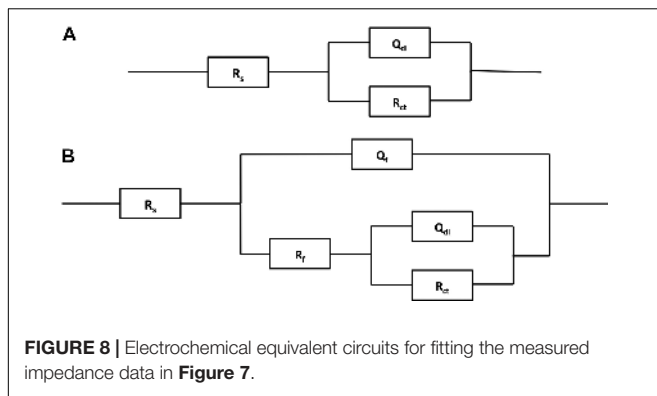
FIGURE 7 | Nyquist and Bode diagrams of the impedance measurements of different electrodes in the *Pseudomonas aeruginosa*-inoculated culture medium as a function of time. **(A,B)** 304L BM, **(C,D)** 304L WZ, **(E,F)** 304L-Cu BM, and **(G,H)** 304L-Cu WZ. The black solid lines are fitting impedance curves with proper equivalent circuits in **Figure 8**. BM, base metal; WZ, welding zone.

FIGURE 8 | Electrochemical equivalent circuits for fitting the measured impedance data in **Figure 7**.

FIGURE 9 | Potentiodynamic polarization curves of various 304L SS electrodes after 14 days of immersion in the 2216E culture medium with *Pseudomonas aeruginosa*. SS, stainless steel.

the resistance to pitting corrosion and the I_{corr} value indicates the stability of passive film on the surface of SS, the two Cu-bearing electrodes showed better pitting corrosion and uniform corrosion resistance against *P. aeruginosa*. 304L-Cu BM showed the highest E_{pit} value (398.1 mV/SCE) among four electrodes. The I_{corr} values of 304L-Cu WZ and 304L BM were close, which were 305.9 and 399.0 nA/cm^2, respectively. However, the E_{pit} of 304L-Cu WZ (346.2 mV/SCE) was higher than that of 304L BM (302.0 mV/SCE). The I_{corr} and E_{pit} values for 304L SS WZ were 877.0 and 212.8 mV/SCE, respectively, indicating the worst resistance to both pitting and uniform corrosion attack.

DISCUSSION

Effects of Cu Addition and Tungsten Inert Gas Welding on Corrosion Resistance of 304L SS

The effects of microstructural changes in austenitic 304L SS by the processes of TIG welding and Cu addition on the corrosion behaviors are presented in **Figure 2** and **Table 2**. Under the testing condition (3.5% NaCl), the high concentration of chloride ions was the main cause for the corrosion (Lu et al., 2005). According to the difference between 304L BM and 304L-Cu BM, the Cu addition slightly improved the uniform corrosion resistance of the austenitic SS, which was proved by decrease of the I_{corr} value. The previous works reported that the moderate amount of Cu addition in SSs could improve the corrosion resistance (Ishu et al., 2011). The dissolved copper ions could react with the chloride ions in solution on the material surface, and their reaction product $CuCl_2$ could work as a protective film. However, at the high potential region, the E_{pit} of 304L BM was appreciably reduced by Cu addition, and the I_{pass} was also increased, implying that Cu addition might weaken the compactness of passive film and then reduce the pitting resistance of 304L BM in the solution with a high concentration of chloride ions (Gui et al., 2016).

According to **Figure 2** and **Table 2**, the 304L WZ possessed lower pitting resistance and uniform corrosion resistance with higher I_{pass} and lower E_{pit} than did the 304L BM. Similarly, the corrosion resistance of 304L-Cu WZ was worse than that of 304L-Cu BM. That indicated that the TIG welding process decreases
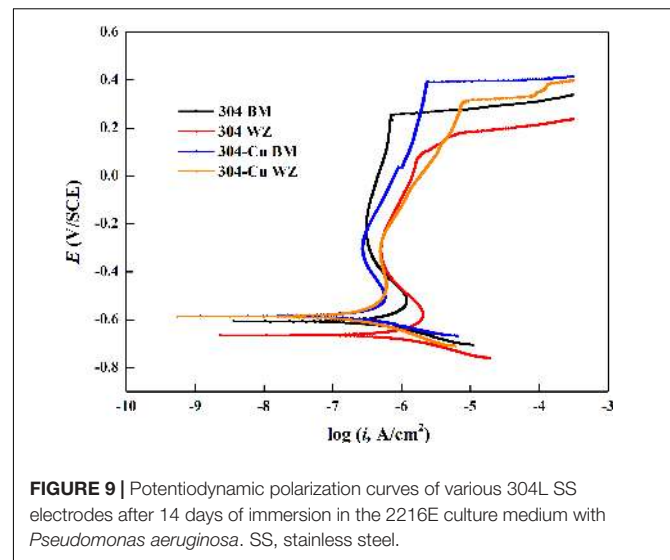
the anticorrosive property and that WZ is prone to the occurrence of the pitting corrosion. It is mainly due to the overquick cooling process after welding, the diffusion of the alloying elements was suppressed, and therefore those elements were nonuniformly distributed in WZs (Dadfar et al., 2007). Besides, in comparison with BM, WZ has more negative E_{corr} value. Thus, when BM and WZ were adjacently placed together in a corrosive environment, the WZ (with the welding parameters as mentioned above) served as a corrosive weakness and decreases the service safety.

Resistance of Cu-Bearing Stainless Steel Against *Pseudomonas aeruginosa*-Induced Corrosion

As shown in **Figure 6A**, the sharp decline of each OCP curves in the initial stage may be induced by the formation of *P. aeruginosa* biofilm, which changed the interface state between the corrosive environment and the passive film of electrodes. It should be noted that the rising tendency of OCP curves was observed in all I_{corr} curves even in the initial stage. Those changes were attributed to the acceleration of anodic reaction induced by *P. aeruginosa* sessile cells. According to the researches on the corrosion mechanism induced by *P. aeruginosa*, the formation of biofilm on the metal surface is crucial to the biocorrosion. In the process of biofilm formation and growth, the extracellular polymeric substances (EPSs) secreted by sessile cells are essential (Pillay and Lin, 2013). Pyocyanin is one of the EPSs of *P. aeruginosa*, which can serve as the electron carrier and participate in the extracellular electron transport (EET) mechanism (Rabaey et al., 2004). In EET-MIC, the sessile cells in biofilms use the energetic metal (e.g., Fe) as the electron donor and the non-oxygen oxidant as the electron acceptor. However, the reduction of this oxidant has occurred inside the sessile cells' cytoplasm because the reaction requires biocatalysts by intracellular enzymes (Jia et al., 2019). Owing to the iron oxidation that occurs extracellularly, the electron carrier (pyocyanin for *P. aeruginosa*) is needed

to transport extracellular electrons to the cytoplasm for the reduction reaction. As a result, the whole process of EET leads to the depolarization and seriously accelerates the corrosion rate. The impedance plots in **Figure 7** also confirm that the reaction on steel electrodes was accelerated owing to the existence of the *P. aeruginosa* biofilm.

However, the Cu-bearing specimens have strong antibacterial property. As shown in **Figures 3**, **4**, the Cu-bearing specimens significantly inhibited the *P. aeruginosa* biofilm formation and killed most of sessile cells. The excellent antibacterial property of 304L-Cu BM and 304L-Cu WZ is due to the release of Cu^+ and Cu^{2+} ions during corrosion process. Both Cu^+ and Cu^{2+} ions are highly toxic to *P. aeruginosa* cells. The main bactericidal mechanism of Cu^+ and Cu^{2+} is the adherence to the cytomembrane and cytoderm of bacteria and the damage of the intracellular protein of bacterial cells (Elguindi et al., 2011; Santo et al., 2011; Zhang et al., 2020).

Because of the protective effect of copper ions, both 304L-Cu BM and 304L-Cu WZ electrodes show a much better anticorrosive property than 304L BM and 304L WZ in the *P. aeruginosa* culture medium. This protection mechanism also works on the localized corrosion attack induced by *P. aeruginosa* biofilm. Previous research revealed that the non-uniform distributed *P. aeruginosa* biofilm can locally decrease the pH value at the interface, which is one of the main reasons to cause pitting corrosion (Hamzah et al., 2013; Li et al., 2016). As the biofilm cannot grow well on the surface of 304L-Cu BM and 304L-Cu WZ specimens, these Cu-bearing specimens had higher E_{pit} values and smaller pit depths, as shown in **Figures 5**, **9**. The results in **Figure 2** also indicated that the Cu addition causes a remarkable inhibition effect on the MIC-induced pitting corrosion. Besides, the pits' shape (shown in **Figure 5**) has little difference between 304L SS and 304L-Cu SS specimens. It can be inferred that the protective effect of Cu only works by killing the corrosive bacteria, which slows down the accelerated EET-MIC steps.

CONCLUSION

(1) After the welding treatment, the Cu addition had no obvious effect on the microstructure, which was composed of complete austenite grains in BM and the dendritic austenite matrix with small amount of δ-ferrite in WZs.
(2) The formation of biofilm was inhibited on the surface of 304L-Cu BM and 304L-Cu WZ.
(3) The MIC resistance of 304L SS was significantly improved by Cu addition. The resistance against uniform and pitting corrosion of 304L-Cu WZ was even much higher than that of 304L BM in *P. aeruginosa* culture medium.

DATA AVAILABILITY STATEMENT

All datasets generated for this work are included in the article/supplementary material.

AUTHOR CONTRIBUTIONS

CY and KY designed this work. LY, JZ, HZ, and YS prepared and characterized the samples. LY and TX cowrote the manuscript. CY revised the manuscript. All authors listed have made a substantial, direct and intellectual contribution to the work, and approved it for publication.

FUNDING

REFERENCES

Aktas, D. F., Lee, J. S., Little, B. J., Ray, R. I., Davidova, A. I., Lyles, C. N., et al. (2010). Anaerobic metabolism of biodiesel and its impact on metal corrosion. *Energ. Fuel.* 24, 2924–2928. doi: 10.1021/ef100084j

Dadfar, M., Fathi, M. H., Karimzadeh, F., Dadfar, M. R., and Saatchi, A. (2007). Effect of TIG welding on corrosion behavior of 316L stainless steel. *Mater. Lett.* 61, 2343–2346. doi: 10.1016/j.matlet.2006.09.008

Elguindi, J., Moffitt, S., Hasman, H., Andrade, C., Raghavan, S., and Rensing, C. (2011). Metallic copper corrosion rates, moisture content, and growth medium influence survival of copper ion-resistant bacteria. *Appl. Microbiol. Biotechnol.* 89, 1963–1970. doi: 10.1007/s00253-010-2980-x

Gui, Y., Zheng, Z. J., and Gao, Y. (2016). The bi-layer structure and the higher compactness of a passive film on nanocrystalline 304 stainless steel. *Thin Solid Films* 599, 64–71. doi: 10.1016/j.tsf.2015.12.039

Hamzah, E., Hussain, M. Z., Ibrahim, Z., and Abdolahi, A. (2013). Influence of *Pseudomonas aeruginosa* bacteria on corrosion resistance of 304 stainless steel. *Corros. Eng. Sci. Technol.* 48, 116–120. doi: 10.1179/1743278212Y.0000000052

Hashemi, S. J., Bak, N., Khan, F., Hawboldt, K., Lefsrud, L., and Wolodko, J. (2018). Bibliometric analysis of microbiologically influenced corrosion (MIC) of oil and gas engineering systems. *Corrosion* 74, 468–486. doi: 10.5006/2620

Huttunen-Saarivirta, E., Honkanen, M., Lepisto, T., Kuokkala, V. T., Koivisto, L., and Berg, C. G. (2012). Microbiologically influenced corrosion (MIC) in stainless steel heat exchanger. *Appl. Surf. Sci.* 258, 6512–6526. doi: 10.1016/j.apsusc.2012.03.068

Ishu, T., Ujiro, T., Hamada, E., Ishikawa, S., and Kato, Y. (2011). A mechanism of improvement in the corrosion resistance of ferritic stainless steels by Cu addition. *Tetsu To Hagane* 97, 441–449.

Jia, R., Unsal, T., Xu, D. K., Lekbach, Y., and Gu, T. Y. (2019). Microbiologically influenced corrosion and current mitigation strategies: a state of the art review. *Int. Biodeterior. Biodegrad.* 137, 42–58. doi: 10.1016/j.ibiod.2018.11.007

Jiang, J., Xu, D. K., Xi, T., Shahzad, M. B., Khan, M. S., Zhao, J. L., et al. (2016). Effects of aging time on intergranular and pitting corrosion behavior of Cu-bearing 304L stainless steel in comparison with 304L stainless steel. *Corrosion Sci.* 113, 46–56. doi: 10.1016/j.corsci.2016.10.003

Jin, S. J., Ren, L., and Yang, K. (2016). Bio-functional cu containing biomaterials: a new way to enhance bio-adaption of biomaterials. *J. Mater. Sci. Technol.* 32, 835–839. doi: 10.1016/j.jmst.2016.06.022

Li, H. B., Yang, C. T., Zhou, E. Z., Yang, C. G., Feng, H., Jiang, Z. H., et al. (2017). Microbiologically influenced corrosion behavior of S32654 super austenitic stainless steel in the presence of marine *Pseudomonas aeruginosa* biofilm. *J. Mater. Sci. Technol.* 33, 1596–1603. doi: 10.1016/j.jmst.2017.03.002

Li, H. B., Zhou, E. Z., Ren, Y. B., Zhang, D. W., Xu, D. K., Yang, C. G., et al. (2016). Investigation of microbiologically influenced corrosion of high nitrogen nickel-free stainless steel by *Pseudomonas aeruginosa*. *Corrosion Sci.* 111, 811–821. doi: 10.1016/j.corsci.2016.06.017

Li, M. J., Nan, L., Xu, D. K., Ren, G. G., and Yang, K. (2015). Antibacterial performance of a Cu-bearing stainless steel against microorganisms in tap water. *J. Mater. Sci. Technol.* 31, 243–251. doi: 10.1016/j.jmst.2014.11.016

Li, Y. C., Xu, D. K., Chen, C. F., Li, X. G., Jia, R., Zhang, D. W., et al. (2018). Anaerobic microbiologically influenced corrosion mechanisms interpreted using bioenergetics and bioelectrochemistry: a review. *J. Mater. Sci. Technol.* 34, 1713–1718. doi: 10.1016/j.jmst.2018.02.023

Liu, H. W., Gu, T. Y., Zhang, G. A., Liu, H. F., and Cheng, Y. F. (2018a). Corrosion of X80 pipeline steel under sulfate-reducing bacterium biofilms in simulated CO_2-saturated oilfield produced water with carbon source starvation. *Corrosion Sci.* 136, 47–59. doi: 10.1016/j.corsci.2018.02.038

Liu, H. W., Sharma, M., Wang, J. L., Cheng, Y. F., and Liu, H. F. (2018b). Microbiologically influenced corrosion of 316L stainless steel in the presence of Chlorella vulgaris. *Int. Biodeterior. Biodegrad.* 129, 209–216. doi: 10.1016/j.ibiod.2018.03.001

Liu, H. W., Xu, D. K., Yang, K., Liu, H. F., and Cheng, Y. F. (2017). Corrosion of antibacterial Cu-bearing 316L stainless steels in the presence of sulfate reducing bacteria. *Corrosion Sci.* 132, 46–55. doi: 10.1016/j.corsci.2017.12.006

Lu, B. T., Chen, Z. K., Luo, J. L., Patchett, B. M., and Xu, Z. H. (2005). Pitting and stress corrosion cracking behavior in welded austenitic stainless steel. *Electrochim. Acta* 50, 1391–1403. doi: 10.1016/j.electacta.2004.08.036

Moon, K. M., Kim, Y. H., Kim, S. J., Yoon, J. H., Lee, Y. C., Lee, S. Y., et al. (2011). Electrochemical Evaluation on the corrosion properties of welding zones of 304 stainless steel. *Adv. Mater. Res.* 146-147, 1238–1242.

Nan, L., Xu, D. K., Gu, T. Y., Song, X., and Yang, K. (2015). Microbiological influenced corrosion resistance characteristics of a 304L-Cu stainless steel against *Escherichia coli*. *Mater. Sci. Eng. C Mater. Biol. Appl.* 48, 228–234. doi: 10.1016/j.msec.2014.12.004

Nan, L., and Yang, K. (2010). Cu ions dissolution from Cu-bearing antibacterial stainless steel. *J. Mater. Sci. Technol.* 26, 941–944. doi: 10.1016/S1005-0302(10)60152-1

Neria-Gonzalez, I., Wang, E. T., Ramirez, F., Romero, J. M., and Hernandez-Rodriguez, C. (2006). Characterization of bacterial community associated to biofilms of corroded oil pipelines from the southeast of Mexico. *Anaerobe* 12, 122–133. doi: 10.1016/j.anaerobe.2006.02.001

Nie, F. L., Wang, S. G., Wang, Y. B., Wei, S. C., and Zheng, Y. F. (2011). Comparative study on corrosion resistance and in vitro biocompatibility of bulk nanocrystalline and microcrystalline biomedical 304 stainless. *Dent. Mater.* 27, 677–683. doi: 10.1016/j.dental.2011.03.009

Pillay, C., and Lin, J. (2013). Metal corrosion by aerobic bacteria isolated from stimulated corrosion systems: effects of additional nitrate sources. *Int. Biodeterior. Biodegrad.* 83, 158–165. doi: 10.1016/j.ibiod.2013.05.013

Pouranvari, M., Alizadeh-Sh, M., and Marashi, S. P. H. (2015). Welding metallurgy of stainless steels during resistance spot welding part I: fusion zone. *Sci. Technol. Weld. Join* 28, 502–511. doi: 10.1179/1362171815Y.0000000015

Rabaey, K., Boon, N., Siciliano, S. D., Verhaege, M., and Verstraete, W. (2004). Biofuel cells select for microbial consortia that self-mediate electron transfer. *Appl. Environ. Microbiol.* 70, 5373–5382. doi: 10.1128/AEM.70.9.5373-5382.2004

Santo, C. E., Lam, E. W., Elowsky, C. G., Quaranta, D., Domaille, D. W., Chang, C. J., et al. (2011). Bacterial killing by dry metallic copper surfaces. *Appl. Environ. Microbiol.* 77, 794–802. doi: 10.1128/AEM.01599-10

Skovhus, T. L., Eckert, R. B., and Rodrigues, E. (2017). Management and control of microbiologically influenced corrosion (MIC) in the oil and gas industry-overview and a North Sea case study. *J. Biotechnol.* 256, 31–45. doi: 10.1016/j.jbiotec.2017.07.003

Sun, Y. P., Yang, C. T., Yang, C. G., Xu, D. K., Li, Q., Yin, L., et al. (2019). Stern–geary constant for X80 pipeline steel in the presence of different corrosive microorganisms. *Acta Metall. Sin. (Engl. Lett.)* 32, 1483–1489. doi: 10.1007/s40195-019-00902-6

Vigneron, A., Alsop, E. B., Chambers, B., Lomans, B. P. I, Head, M., and Tsesmetzis, N. (2016). Complementary microorganisms in highly corrosive biofilms from an offshore oil production facility. *Appl. Environ. Microb.* 82, 2545–2554. doi: 10.1128/AEM.03842-15

Wadood, H. Z., Rajasekar, A., Ting, Y. P., and Sabari, A. N. (2017). Role of *Bacillus subtilis* and *Pseudomonas aeruginosa* on corrosion behavior of stainless steel. *Arab. J. Sci. Eng.* 40, 1825–1836. doi: 10.1007/s13369-015-1590-4

Xi, T., Shahzad, M. B., Xu, D. K., Sun, Z. Q., Zhao, J. L., Yang, C. G., et al. (2017). Effect of copper addition on mechanical properties, and antibacterial property of 316L stainless steel corrosion resistance. *Mater. Sci. Eng. C Mater. Biol. Appl.* 71, 1079–1085. doi: 10.1016/j.msec.2016.11.022

Xi, T., Shahzad, M. B., Xu, D. K., Zhao, J. L., Yang, C. G., Qi, M., et al. (2016). Copper precipitation behavior and mechanical properties of Cu-bearing 316L austenitic stainless steel: a comprehensive cross-correlation study. *Mater. Sci. Eng. A Struct. Mater.* 675, 243–252. doi: 10.1016/j.msea.2016.08.058

Xu, D. K., Xia, J., Zhou, E. Z., Zhang, D. W., Li, H. B., Yang, C. G., et al. (2017a). Accelerated corrosion of 2205 duplex stainless steel caused by marine aerobic *Pseudomonas aeruginosa* biofilm. *Bioelectrochemistry* 113, 1–8. doi: 10.1016/j.bioelechem.2016.08.001

Xu, D. K., Zhou, E. Z., Zhao, Y., Li, H. B., Liu, Y. Z., Zhang, D. W., et al. (2017b). Enhanced resistance of 2205 Cu-bearing duplex stainless steel towards microbiologically influenced corrosion by marine aerobic *Pseudomonas aeruginosa* biofilms. *J. Mater. Sci. Technol.* 34, 1325–1336. doi: 10.1016/j.jmst.2017.11.025

Zhang, D., Ren, L., Zhang, Y., Xue, N., Yang, K., and Zhong, M. (2013). Antibacterial activity against *Porphyromonas gingivalis* and biological characteristics of antibacterial stainless steel. *Colloid Surf. B Biointerfaces* 105, 51–57. doi: 10.1016/j.colsurfb.2012.12.025

Zhang, P. Y., Xu, D. K., Li, Y. C., Yang, K., and Gu, T. Y. (2015). Electron mediators accelerate the microbiologically influenced corrosion of 304 stainless steel by the *Desulfovibrio vulgaris* biofilm. *Bioelectrochemistry* 101, 14–21. doi: 10.1016/j.bioelechem.2014.06.010

Zhang, X. R., Yang, C. G., and Yang, K. (2020). Contact killing of Cu-bearing stainless steel based on charge transfer caused by the microdomain potential difference. *ACS Appl. Mater. Inter.* 12, 361–372. doi: 10.1021/acsami.9b19596

Conflict of Interest: The authors declare that the research was conducted in the absence of any commercial or financial relationships that could be construed as a potential conflict of interest.